Separation Science and Technology
Publication details, including instructions for authors and subscription information:
http://www.informaworld.com/smpp/title~content=t713708471

Outlet Streams Swing (OSS) and MultiFeed Operation of Simulated Moving Beds

Pedro Sá Gomes[a]; Alírio E. Rodrigues[a]
[a] Laboratory of Separation and Reaction Engineering (LSRE), Department of Chemical Engineering-Faculty of Engineering, University of Porto, Porto, Portugal

To cite this Article Gomes, Pedro Sá and Rodrigues, Alírio E.(2007) 'Outlet Streams Swing (OSS) and MultiFeed Operation of Simulated Moving Beds', Separation Science and Technology, 42: 2, 223 — 252
To link to this Article: DOI: 10.1080/01496390601070125
URL: http://dx.doi.org/10.1080/01496390601070125

Separation Science and Technology, 42: 223–252, 2007

ISSN 0149-6395 print/1520-5754 online
DOI: 10.1080/01496390601070125

Outlet Streams Swing (OSS) and MultiFeed Operation of Simulated Moving Beds

Pedro Sá Gomes and Alírio E. Rodrigues
Laboratory of Separation and Reaction Engineering (LSRE), Department of Chemical Engineering–Faculty of Engineering, University of Porto, Porto, Portugal

Abstract: A new simulated moving bed (SMB) operation technique is introduced, the outlet streams swing (OSS), based on the dynamic collection of fronts from the equivalent true moving bed (TMB). This new assumption improves the product outlet purities, when compared with the classic operating mode, as a consequence of an increased separation between collection fronts and the contaminating ones. The strategy is dynamic and discontinuous, a collection front expansion is performed in zone 1 and/or 4, obtained by the violation of the classic respective design constraints during a first step and contraction during the second step using at least the classic design operating parameter for zones 1 and 4.

Another non-conventional technique, the MultiFeed (MF) SMB operation, is simulated and analyzed here as a solo technique as well as a powerful modelling technique for the particular case of inner sections Varicol® (only the zones 2 and 3 have variable number of columns).

Keywords: Outlet streams swing, OSS, MultiFeed, MF, simulated moving bed, SMB, chiral separation, modelling and simulation

INTRODUCTION

The simulated moving bed (SMB) was first developed by the universal oil products (UOP) (1), with the Sorbex® processes, as a practical solution to

Received 11 April 2006, Accepted 2 October 2006
Address correspondence to Alírio E. Rodrigues, Laboratory of Separation and Reaction Engineering (LSRE), Department of Chemical Engineering–Faculty of Engineering, University of Porto, Rua Dr. Roberto Frias s/n, 4200-465 Porto, Portugal. E-mail: arodrig@fe.up.pt

the counter-current true moving bed (TMB), avoiding the problems observed when solid motion is present, by simulating it with a syncronous port shifting while keeping the solid immobile. Appearing predominantly in the large separations associated with the petrochemical industry as for the separation of the *p*-xylene (Eluxyl® process (2, 3), the SMB technology experimented an emergent interest in the last decade principally with its application to drugs separation in the pharmaceutical industry as in chiral separations (4–7), or in other fields as biotechnological and fine chemistry products separation and recovery.

This late demand on the SMB technique is directly linked to research efforts, leading to the formulation of quite different operation modes since the original patent. Non conventional strategies as the introduction of non-synchronous inlet/outlet shifts, the Varicol® process (8, 9) or the variable flow with/or variable composition in the inlet/outlet streams, the PowerFeed process (10, 11) and Modicon (12, 13), as well as the utilization of multiple feed or distributed feed (the Two Feeds SMB in (14), have increased the potential of this technique for a vast range on the binary separation field.

For multiple component separation is from "common wisdom" the utilization of several SMB units in cascade to obtain each product to a certain degree of purity and some cascade configurations have been studied and proposed; nevertheless, new advances have also been made in this domain, as keeping the four zones either by alternating two different adsorbents (15), two different solvents (16), or having a variation of the working flow rates during the switching period were also proposed (17). Five-zone SMB with a third fraction withdrawn from the system besides products of extract and raffinate were also discussed (18). Recently, a single cascade SMB system was investigated for ternary separation, which is especially suitable for a system with a little amount of the most strongly adsorbed component and a significant amount of the middle component (19). Kishihara et al. (20) proposed a 9-zone SMB which considers a 4-zone and 5-zone rings connected in parallel, where internal bypass stream with partially separated mixture is introduced from one ring to the other. Similarly Wooley et al. (21) proposed a 9-zone system for glucose and xylose recovery from biomass hydrolyzate. The ternary separation process that operates in two steps (22) was commercialized by Organo Corp. and modelled as pseudo-SMB (23) and (24); in the first step the feed is loaded and the intermediate component is collected being all unit working as a fixed bed, and in the second step the feed is stopped and the other two components are collected, now operating as an SMB.

The aim of this work is the simulation of two non-conventional SMB techniques: one, outlet streams swing (OSS) technique here firstly presented, is based on the concept of dynamic collection fronts in the equivalent TMB model leading to extract and raffinate streams enrichment by increasing their purities in the real SMB units; the other, MultiFeed (MF) SMB, presents a

new tool on Varicol® SMB modelling/optimization techniques as a different non-conventional SMB operation technique analogous to multiple feed distillation columns, similar to the one introduced by Kim et al. (14) in the particular case of the Two–Feed SMB.

MODELLING STRATEGIES

The TMB model is often used for studies in the SMB field, presenting in fact a reasonable agreement with the experimental data when a large number of columns are considered. The main advantage for the modelling of a TMB instead of the SMB lies in the different level of difficulty involved in the solution of the two strategies and the time required to perform their computation. Nevertheless, the two modelling strategies are used here, first by simulating the system directly (here called as Real SMB), taking into account its intermittent behavior, and secondly by representing its operation in terms of a true counter-current system (referred in this work as Equivalent TMB).

Real SMB

Due to the switch of inlet and outlet streams, each column plays a different role during an entire cycle, depending on its location. In this way for the real SMB model, after each switch interval all the boundary conditions for each of the columns are synchronously changed, but always respecting the intersection nodes mass balances,

- $j = 1: C_{bi(4,x=1)} = \dfrac{u_1^*}{u_4^*} C_{bi(1,x=0)}$ Eluent node (1a)
- $j = 2, 4: C_{bi(j-1,x=1)} = C_{bi(j,x=0)}$ Extract, and Raffinate nodes (1b)
- $j = 3: C_{bi(2,x=1)} = \dfrac{u_3^*}{u_2^*} C_{bi(3,x=0)} - \dfrac{u_F}{u_2^*} C_i^F$ Feed node (1c)

where,

- $u_1^* = u_4^* + u_E$ Eluent (E) node (2a)
- $u_2^* = u_1^* - u_X$ Extract (X) node (2b)
- $u_3^* = u_2^* + u_F$ Feed (F) node (2c)
- $u_4^* = u_3^* - u_R$ Raffinate (R) node (2d)

with u_j^* representing the section j interstitial velocity in the real SMB equipment, C_{bij} species i bulk concentration in j section and C_i^F the species i feed inlet concentration.

This time-dependence of the boundary conditions leads to a cyclic steady-state (CSS), instead of the real steady-state achieved for the true counter current model, TMB. In this work a result from a dynamic simulation is considered to be at the CSS when the difference between the same variable in two consecutives switches is less than 2.5%, as well as the global mass balance has been verified with an error tolerance less than 5%.

It is possible to simulate the real SMB using a more complete model, detailing the particle diffusion and/or film mass transfer (the detailed particle model) as stated for TMB reactive systems in (25), or by approximation to the intraparticle mass transfer averaging the intraparticle concentration and introducing the linear driving force (LDF) concept as mentioned by Glueckauf (26). This second methodology has proved to be quite accurate with the reproduction of experimental results and has been used in the majority of the published work in the field. In this work it will only be applied to the LDF approach, considering a convective fluid movement with axial dispersion, negligible thermal effects, constant values for the bed void fraction ε_b, particle radius R_p, axial dispersion coefficient D_{bj}, particle radius R_p, particle effective diffusion D_{pei}, constant values for the flow rates/interstitial velocities in each section, and also a negligible pressure drop.

Therefore transient mass balances are performed to each species i in each column c, and in the molar basis it becomes:

1. In a volume element of the bulk fluid phase,

$$\frac{\partial C_{bic}}{\partial \theta} = \gamma_j^* \left\{ \frac{1}{Pe_c} \frac{\partial^2 C_{bic}}{\partial x^{*2}} - \frac{\partial C_{bic}}{\partial x^*} \right\} - \frac{(1-\varepsilon_b)}{\varepsilon_b} k^*_{p_{ic}} \left(q^*_{ic} - \langle q_{ic} \rangle \right) \tag{3}$$

2. and to the bed "solid-phase",

$$\frac{d\langle q_{ic} \rangle}{d\theta} = k^*_{p_{ic}} (q^*_{ic} - \langle q_{ic} \rangle) \tag{4}$$

with the initial and the Danckwerts boundary conditions (27), previously mentioned in Langmuir work (28),

- $$\begin{cases} C_{ic}(x^*, 0) = 0; \\ \langle q_{ic}(x^*, 0) \rangle = 0; \end{cases} \tag{5}$$
- $$x^* = 0 \colon C_{bic}(0^-, \theta) = C_{bic}(0, \theta) - \frac{1}{Pe_c} \left. \frac{\partial C_{bic}}{\partial x^*} \right|_{x^*=0}, \; c = 1 \text{ to } NC \tag{6a}$$
- $$x^* = 1 \colon \left. \frac{\partial C_{bic}}{\partial x^*} \right|_{x^*=1} = 0 \tag{6b}$$

and the adsorption equilibrium isotherm defined as:

$$q_{ic}^{*} = f_i(C_{bic}, C_{bkc}) \text{ with } k \neq i \text{ and for all species } i \tag{7}$$

where $C_{bic}(0^{-}, \theta)$ represents the species i column c inlet concentration, $\theta = t/t_c$ is the dimensionless time normalized by the SMB ports switch time t_c, $x^{*} = z/L_c$; $\gamma_j^{*} = u_j^{*}/u_s$ the ratio between fluid and equivalent solid interstitial velocities, $Pe_c^{*} = u_j^{*}L_c/D_{bj}$ the Peclet number, and $k_{p_{ic}}^{*} = (\Psi D_{pei}/R_p^2)t_c = k_{LDF} \cdot t_c$ the number of intraparticle mass transfer units with k_{LDF} the LDF mass transfer coefficient, where Ψ a coefficient between 10 and 15.

Equivalent TMB

It is possible to establish the correspondence between SMB and an equivalent TMB model by the introduction of the relative velocity concept $u_j^{*} = u_j + u_s$, where u_j is the fluid interstitial velocity in the equivalent TMB model, and considering that the solid velocity in the TMB (representing the counter-current solid motion), is evaluated from the switch time interval value t_c in the real SMB model as $u_s = L_c/t_c$, what implies that the internal flow-rates in both models are not the same, but related by $Q_j^{*} = Q_j + \varepsilon_b V_c/t_c$, where Q_j^{*} and Q_j represent the internal liquid flow-rates in the SMB and TMB models respectively, and V_c the column volume. Leading to the equivalent nodes balances,

- $j = 1: C_{bi(4,x=1)} = \dfrac{u_1}{u_4} C_{bi(1,x=0)}$ Eluent node (8a)
- $j = 2, 4: C_{bi(j-1,x=1)} = C_{bi(j,x=0)}$ Extract and raffinate nodes (8b)
- $j = 3: C_{bi(2,x=1)} = \dfrac{u_3}{u_2} C_{bi(3,x=0)} - \dfrac{u_F}{u_2} C_i^{F}$ Feed node (8c)

and,

- $u_1 = u_4 + u_E$ Eluent node (9a)
- $u_2 = u_1 - u_X$ Extract node (9b)
- $u_3 = u_2 + u_F$ Feed node (9c)
- $u_4 = u_3 - u_R$ Raffinate node (9d)

1. Again for the bulk fluid mass balance,

$$\frac{\partial C_{bij}}{\partial \theta} = \frac{\gamma_j}{n_j}\left\{\frac{1}{Pe_j}\frac{\partial^2 C_{bij}}{\partial x^2} - \frac{\partial C_{bij}}{\partial x} - \frac{(1-\varepsilon_b)}{\varepsilon_b} k_{p_{ij}}\left(q_{ij}^{*} - \langle q_{ij}\rangle\right)\right\} \tag{10}$$

2. and for bed mass balance,

$$\frac{\partial \langle q_{ij} \rangle}{\partial \theta} = \frac{1}{n_j} \frac{\partial \langle q_{ij} \rangle}{\partial x} + \frac{\gamma_j}{n_j} k_{p_{ij}} \left(q_{ij}^* - \langle q_{ij} \rangle \right) \tag{11}$$

with the initial and boundary conditions,

- $$\begin{cases} C_{bij}(x, 0) = 0; \\ \langle q_{ij}(x, 0) \rangle = 0; \end{cases} \tag{12}$$
- $$x = 0 \colon C_{bi(j,x=0)} = C_{bij}(0, \theta) - \frac{1}{Pe_j} \left. \frac{\partial C_{bij}}{\partial x} \right|_{x=0} \tag{13a}$$
- $$x = 1 \colon \left. \frac{\partial C_{bij}}{\partial x} \right|_{x=1} = 0 \tag{13b}$$

and

- $$x = 1 \begin{cases} \langle q_{ij} \rangle = \langle q_{i(j+1,x=0)} \rangle, & \text{for } j = 1, 2, 3; \\ \langle q_{i4} \rangle = \langle q_{i(1,x=0)} \rangle \end{cases} \tag{14}$$

where $x = z/L_j$ the dimensionless column axial coordinate with respect to the length of zone j, $L_j = L_c\, n_j$; $\gamma_j = u_j/u_s$ the ratio between fluid and solid interstitial velocities, $Pe_j = u_j L_j / D_{bj}$ the Peclet number, with $t_j = L_j/u_j$ the fluid phase space time; and $k_{p_{ij}} = \Psi D_{pei}/R_p^2\, t_j = k_{LDF} \cdot t_j$. plus the adsorption equilibrium isotherm as in (7), but now defined for each section j.

Analysed Cases and Numerical Solution

The different model equations were numerically solved using the gPROMS v2.3.6 a commercial package from Process Systems Enterprise (www.psenterprise.com). The mathematical models are composed by systems of PDE (partial differential equations), ODE (ordinary differential equations), and AE (algebraic equations), that were solved by applying one of the discretization methods available with gPROMS, namely OCFEM (orthogonal collocation on finite elements) with 2 collocation points per element, and 50 elements in each column for the axial coordinate. After the axial discretization step, the time integration is performed by the ordinary differential equation solver SRADAU a fully-implicit Runge-Kutta method that implements a variable time step, the resulting system is then solved by the gPROMS BDNSOL (Block decomposition nonlinear solver).

The SMB outlet/inlet flow rates must satisfy purity and recovery specifications, and performance parameters. The definitions of extract purity (P_X, %), raffinate purity (P_R, %), recovery of the more retained product in the extract (Re c_X^A, %), recovery of the less retained in the raffinate (Re c_R^B, %), and the unit productivity in terms of A in the extract (Pr o_X^A) or B in raffinate (Pr o_R^B), each SMB unit performance, in terms of TMB model

variables (for SMB it should be used the average bulk species concentration over a Switch), are:

$$\mathrm{P}_X(\%) = \frac{C^X_{b_A}}{C^X_{bA} + C^X_{bB}} \times 100$$

$$\mathrm{Rec}^A_X(\%) = \frac{Q_X C^X_{bA}}{Q_F C^F_A} \times 100$$

$$\mathrm{Pr}\, o^A_X = \frac{Q_X C^X_{bA}}{V_{bed}} = \frac{\mathrm{Rec}^A_X \cdot Q_F C^F_A}{V_{bed}}$$

Similar definitions hold for the purity of the raffinate, for the recovery of *B* in the raffinate and for productivity on the raffinate.

As a test case here are considered two different references: for the OSS technique the case of chiral separation system studied by Rodrigues and Pais (7) a classic [2-2-2-2] SMB unit; and for the MultiFeed apparatus the same system as for Varicol® non-conventional SMB arrangement in Pais and Rodrigues (6). Both papers consider the chromatographic resolution of a racemic mixture of chiral epoxide enantiomers (Sandoz Pharma, Basel, Switzerland), constituted by a system of microcrystalline cellulose triacetate (Merck, Darmstadt, Germany) with an average particle diameter of 45 μm as the chiral stationary phase, and pure methanol as eluent. The adsorption equilibrium isotherms measured at 25°C and represented by the linear plus Langmuir competitive model in terms of retained concentration in the particles, from Rodrigues and Pais (7) as,

$$q^*_{Aj} = 1.35 C_{bAj} + \frac{7.32 \cdot 0.163 C_{bAj}}{1 + 0.163 C_{bAj} + 0.087 C_{bBj}}$$

$$q^*_{Bj} = 1.35 C_{bBj} + \frac{7.32 \cdot 0.087 C_{bBj}}{1 + 0.163 C_{bAj} + 0.087 C_{bBj}}$$

with q^*_{ij} in $g \cdot L^{-1}_{\text{particle}}$ and C_{bij} in $g \cdot L^{-1}$.

THE OSS (OUTLET STREAMS SWING) NOVEL SMB OPERATION TECHNIQUE

The Classical SMB Design

In the classic SMB design is from the common-wisdom the use of the TMB model design parameters on the prediction of SMB operating conditions. The design of a TMB consists in the adjustment of sections flow rates values in a way that the less retained component (B) would be recovered in the raffinate and the more retained one (A) in the extract, avoiding the contamination of the raffinate current with the more retained species and the presence of the less retained one in the extract stream. As a result some

constraints are usually set, expressed in terms of species net fluxes in each section. A fine and well known illustration is the schematic TMB operation diagram with the desired net fluxes for a binary separation as in Fig. 1.

It can be observed that for the recovery of the more retained component in the extract, the species A net flux in Section 1 must be upward, cleaning the adsorbent, while in Sections 2 and 3 downward, removing A from the raffinate and feed zones, and as a consequence the more retained species is directed to the extract collecting port. A similar movement is experimented by the less retained component but now the migration is upwards in Sections 2 and 3 and downwards in Section 4, directing B to the raffinate port, between Sections 3 and 4, and cleaning the eluent in zone 4 to be recycled to Section 1. The general constraints are:

$$\begin{aligned}
&\frac{Q_1 C_{bA1}}{Q_s \langle q_{A1} \rangle} > 1 \\
&\frac{Q_2 C_{bB2}}{Q_s \langle q_{B2} \rangle} > 1 \cap \frac{Q_2 C_{bA2}}{Q_s \langle q_{A2} \rangle} < 1 \\
&\frac{Q_3 C_{bB3}}{Q_s \langle q_{B3} \rangle} > 1 \cap \frac{Q_3 C_{bA3}}{Q_s \langle q_{A3} \rangle} < 1 \\
&\frac{Q_4 C_{bB4}}{Q_s \langle q_{B4} \rangle} < 1
\end{aligned} \qquad \text{(15 a-d)}$$

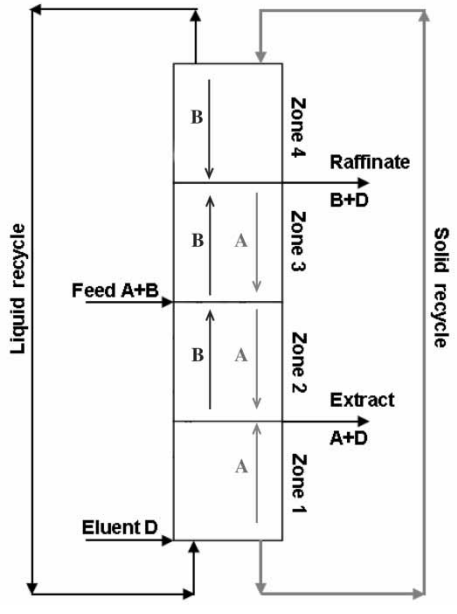

Figure 1. Scheme of an TMB operation diagram with the desired net fluxes for binary separations.

Or considering the ratio between the fluid and the solid interstitial velocities, γ_j as introduced before,

$$\begin{aligned}
\gamma_1 &> \frac{1-\varepsilon_b}{\varepsilon_b}\frac{\langle q_{A1}\rangle}{C_{bA1}} \\
\frac{1-\varepsilon_b}{\varepsilon_b}\frac{\langle q_{B2}\rangle}{C_{bB2}} &< \gamma_2 < \frac{1-\varepsilon_b}{\varepsilon_b}\frac{\langle q_{A2}\rangle}{C_{bA2}} \\
\frac{1-\varepsilon_b}{\varepsilon_b}\frac{\langle q_{B3}\rangle}{C_{bB3}} &< \gamma_3 < \frac{1-\varepsilon_b}{\varepsilon_b}\frac{\langle q_{A3}\rangle}{C_{bA3}} \\
\gamma_4 &< \frac{1-\varepsilon_b}{\varepsilon_b}\frac{\langle q_{B4}\rangle}{C_{bB4}}
\end{aligned} \tag{16a-d}$$

At this point the relation or ratio $\langle q_{ij}\rangle/C_{bij}$ can be treated by one of the two more common strategies. The first one is based on the equilibrium theory, which assumes that the adsorption equilibrium is established everywhere at every time (29–34). It was applied to the TMB design by Storti, Mazzotti, Migliorini, Chiang et al. (35–39) resulting in a feasible separation region formed by the above constraints (15b) and (15c), which takes the form of a rectangular triangle in the ($\gamma_2 \times \gamma_3$) plane, in the case of linear isotherms, or a triangle shaped form with rounded lines in non linear isotherms case. This is, the so-called "Triangle Theory," where the axial mixing as mass transport resistances are neglected. The second strategy is based on the "Separation Volume" method (3, 7, 40, 41), a more complete approach, where all mass transfer resistances are taken into account, plus the optimization is carried out for three different flux zones (2, 3 and 1) or (2, 3 and 4), giving the possibility to the analysis of solvent consumption or a solid recycling, function of the separation zone.

However, both methods will provide constant parameters for the better operation zone in a given TMB design problem, leading to the establishment of static fronts in the different zones of the TMB.

The OSS Modus Operandi

The major and fundamental enhancement presented by this technique lies in the introduction of dynamic fronts in the TMB model, either in the "desorptive" zone 1 or the "adsorptive" zone 4. Instead of collecting the less or more retained components, in raffinate or extract streams respectively at constant concentration, a relative movement is prearranged to these two collection fronts by altering the fluxes in Sections 1 and 4, violating the (15a) and (15d) conditions, while they are kept constant in Sections 2 and 3 as pointed by one of the two theories cited above. Since the parameters are not changed in the inner Sections 2 and 3 the separation remains accurate and minimal the contamination of the outlet streams, i.e., the contamination

fronts in the equivalent TMB model are kept static and away from the collection points.

A simple arrangement of this strategy can be employed to apply it to the two sections at the same time in two different steps: in the first step while the A front in Section 1 is expanding the B front in Section 4 is being contracted, (See Fig. 2(a)) during the second step when the B front in section 4 is expanding the A front in section 1 is being contracted (See Fig. 2(b)), or *vice-versa*.

To induce the (15d) constraint violation, and therefore B front expansion in Section 4, the flux of the raffinate is decreased and the flowrate of the extract is increased, leading to an increase of recycle flow at the end of Section 4, recycled to Section 1 where the contraction of A front is happening. With the decrease of the extract flowrate and increase of the raffinate flow-rate, the opposite movements are observed, with the contraction of the B front in Section 4 at same time that there is an expansion of A front in Section 1.

For linear or quasi linear adsorption isotherms, with products with the same or similar mass transfer rates, the complementarity of A and B fronts expansion/contraction movements is bigger when the selectivity value is near one, i.e., difficult separations. For non linear isotherms the Solute Movement Theory (29), the concentration waves velocities, must also be taken into account in addition to the other effects mentioned above, the selectivity, and the mass transfer rates.

Moving the collection fronts will not change almost anything in the solution of the TMB model. Averaging the concentration variation occurred in the collection port, extract or raffinate node, will result in the same value as if a constant average flow-rate was used, in both zones 1 and 4. But when these types of movements are implemented in a real SMB model, the results are quite different. The collection fronts are stretched or compressed depending on the strategy adopted, if the more retained product is being mainly collected in the extract stream during the first step or in the second step and *vice-versa* for the less retained product in the raffinate.

There is a decrease either in the extract or raffinate flow-rates, this flow-rate decrease is limited by the complete closing of one/both of the mentioned ports. These particular and extreme cases are more detailed later in this work. As mentioned, the OSS operation mode involves two different steps. If the low extract flow-rate and high raffinate flow-rate is occur in the first step, i.e., expansion of a front in section 1 and contraction of B front in Section 2, the canonical "*OSS raffinate-extract*" name is given; otherwise "*OSS extract-raffinate*".

This expansion or contraction of the collection fronts is quite important since the contamination fronts will not suffer from those movements with the same intensity, leading to a decrease or increase of the length between them. The Fig. 3 scheme illustrates the type of induced movements aimed to be obtained in the two collection fronts, simulated by a real SMB model; the strategy here presented is obtained by collecting the more retained

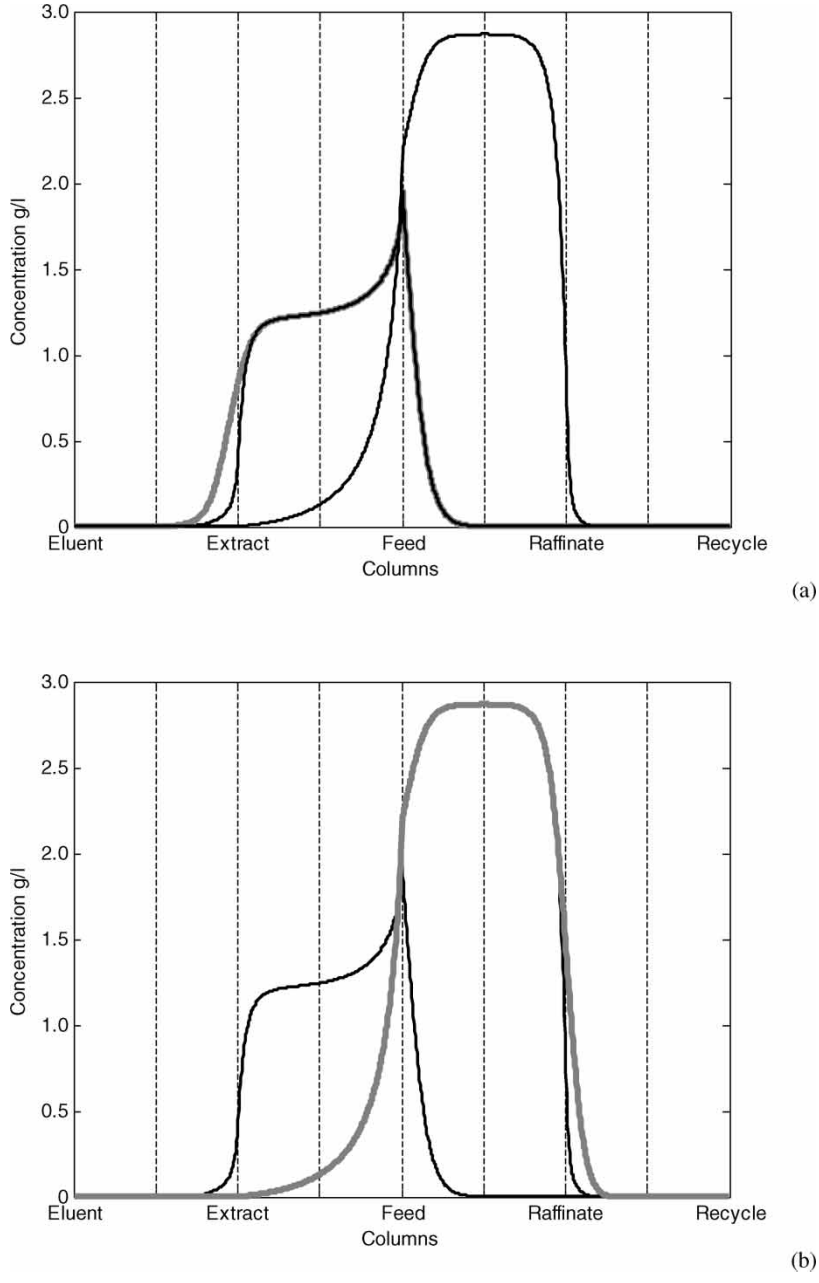

Figure 2. Expansion of front A in section 1 (a), expansion of front in section 4 (b), the black profiles represent A and B concentration as in a classic TMB arrangement, while the grey ones the active OSS technique.

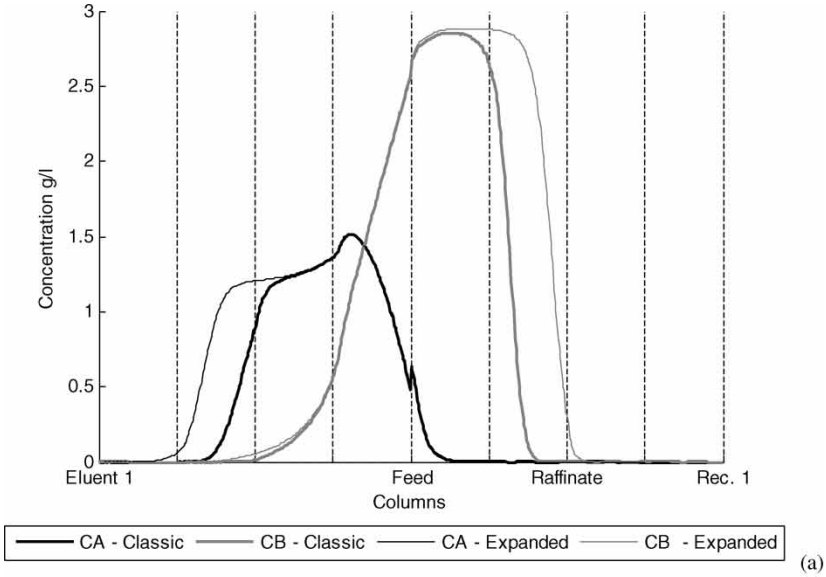

Figure 3. Expansion and contraction movements at cyclic steady state (CSS): (a) at $\theta = 0.25$ and (b) at $\theta = 0.75$.

product (A) in the extract during the second step while the less retained (B) in the raffinate during the first step. In this study each step is performed by half of the time switch (50–50%) not optimized, and the canonical 50–50% OSS *raffinate-extract* name is given.

It should be noted that in Fig. 3 the full line, classic SMB case, the products are always being collected at the end of column 2 (extract point) and at the end of column 6 (raffinate point), while the OSS technique only collects periodically as already mentioned. As can be observed the collection point in Fig. 3(a) is now for product B in the raffinate node while the extract point is closed; the difference between the collection front and the contamination one is larger than the one observed in the classic approach. A similar observation holds for Fig. 3(b) in the extract point. The strategy is dynamic and discontinuous, the expansion either in zone 1 or 4 is obtained by the violation of the respective constraints in each zone ((15a) in zone 1 and (15d) in zone 4). In Fig. 3 the expansion action is performed to the left of the extract point and to the right of the raffinate node, the average of first plus second step flow-rate value to section 1 or 4 must confer the restrictions set by one of the design techniques already mentioned. To calculate the possible collection fronts expansion on real SMB unit it is useful to simulate the dynamic front with its equivalent TMB model, by setting the fluxes to operate the expansion and contraction movements. In the limit once the expansion time reaches the "no return point" the fluxes are set to contraction so that no contamination would be noted in the end of Section 4 or the beginning of Section 1.

A first consequence can be easily noted: for this type of front movements it is necessary to allow some column space, keep the length of the column in

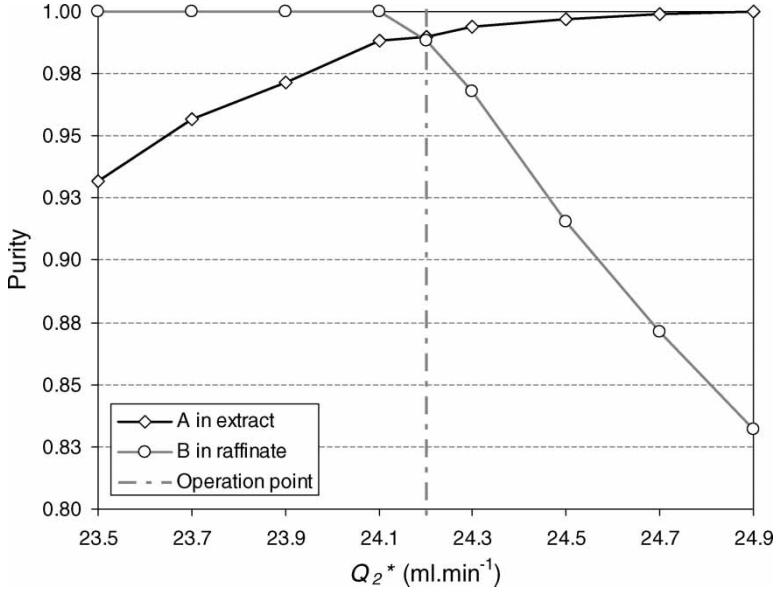

Figure 4. Optimum operating point, for fixed $t_c = 198$ s, $Q_1^* = 33.838\ \text{ml} \cdot \text{min}^{-1}$, $Q_4^* = 21.800\ \text{ml} \cdot \text{min}^{-1}$ and $Q_F = 1.500\ \text{ml} \cdot \text{min}^{-1}$.

Table 1. SMB unit characteristics and model parameters

Model parameters	SMB columns
$Pe_c = 1000$	$N_c = 8 \quad n_j = [2\ 2\ 2\ 2]$
$\varepsilon_b = 0.4$	$L_c = 9.9 \times 10^{-2}$ m
	$R_p = 2.25 \times 10^{-5}$ m
	$d_c = 2.6 \times 10^{-2}$ m
	Classic SMB operating conditions
$k_{LDF} = 0.33\ s^{-1}$	$C_A^F = 5\ g \cdot l^{-1}$
	$C_B^F = 5\ g \cdot l^{-1}$
	$t_c = 198$ s
	$Q_E = 12.038\ ml \cdot min^{-1}$
	$Q_X = 9.638\ ml \cdot min^{-1}$
	$Q_F = 1.500\ ml \cdot min^{-1}$
	$Q_R = 3.900\ ml \cdot min^{-1}$
	$Q_4 = 21.800\ ml \cdot min^{-1}$

Sections 1 and 4 free of products A or B, thus the more column space is available the more extensive the expansion action can perform; as a consequence higher purity of the collected product is obtained, till the limit where the front occupies all of the column available space.

The OSS Technique Simulation

The model parameters and operating conditions, were taken from (7), where the classic interstitial velocity ratios values (γ_j^* or γ_j) for Sections 1 and 4 were kept constant and far from the critical values for total solid and eluent regeneration ($\gamma_1 > \gamma_1^{min} = 3.815$ and $\gamma_4 < \gamma_4^{max} = 2.714$ (7), according to the equilibrium theory), leaving "column space" to perform the OSS technique, not in the lower solvent consumption point. For Sections 2 and 3 the interstitial velocity ratios values were obtained by optimization to the best purity values in extract and raffinate streams for a $1.5\ ml \cdot min^{-1}$ feed inlet Fig. 4, considering the

Table 2. Classic SMB and equivalent TMB section operating conditions

Real SMB	Equivalent TMB
$\gamma_j^* = [5.311\ 3.798\ 4.034\ 3.422]$	$\gamma_j = [4.311\ 2.798\ 3.034\ 2.422]$
$Q_j^* = [33.838\ 24.200\ 25.700$	$Q_j = [27.467\ 17.829\ 19.329$
$21.800]\ ml \cdot min^{-1}$	$15.429]\ ml \cdot min^{-1}$
	$Q_s = 9.557\ ml \cdot min^{-1}$

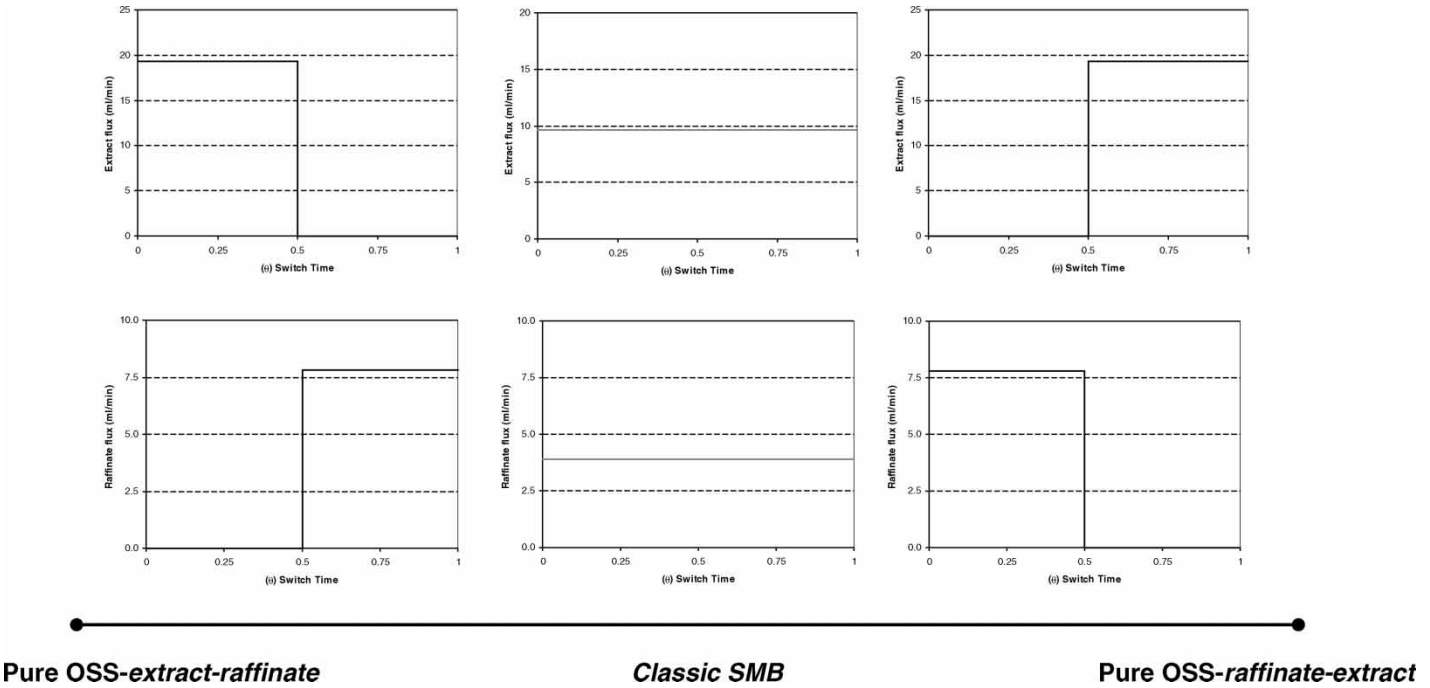

Figure 5. OSS range of application, the pure strategies limits.

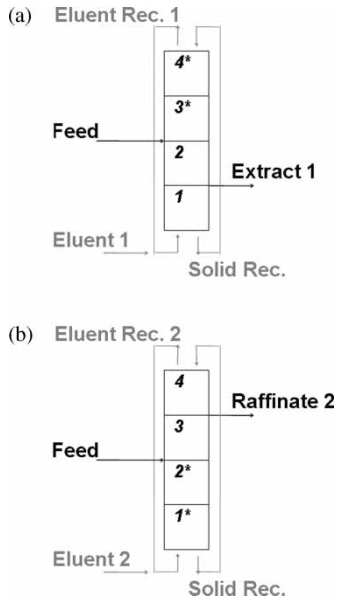

Figure 6. OSS strategy for the test case, (a) the first half of the switch time, (b) the second half of the switch time, equivalent TMB scheme.

mass transfer coefficient of $k_{LDF} = 0.33\ s^{-1}$, and Section 1 and Section 4 constant flow-rates, as in Table 2. By operating at higher or lower solvent consumption values it was found that, for the same feed flow rate, the purity value in both the extract and the raffinate streams was not improved. The full optimized unit, maximum purity, minimum solvent consumption ($Q_E = 8.373\ ml \cdot min^{-1}$) for a given feed flow-rate

Table 3. 50–50% OSS *extract-raffinate* SMB and equivalent TMB section operating conditions

Real SMB 1st half of a θ	Equivalent TMB 1st half of a θ
$\gamma_j^* = [6.824\ 3.798\ 4.034\ 4.034]$ $Q_j^* = [243.476\ 24.200\ 25.700\ 25.700]\ ml \cdot min^{-1}$	$\gamma_j = [5.824\ 2.798\ 3.034\ 3.034]$ $Q_j = [37.105\ 17.829\ 19.329\ 19.329]\ ml \cdot min^{-1}$ $Q_s = 9.557\ ml \cdot min^{-1}$
Real SMB 2nd half of a θ	Equivalent TMB 2nd half of a θ
$\gamma_j^* = [3.798\ 3.798\ 4.034\ 2.809]$ $Q_j^* = [24.200\ 24.200\ 25.700\ 17.900]\ ml \cdot min^{-1}$	$\gamma_j = [2.798\ 2.798\ 3.034\ 1.809]$ $Q_j = [17.829\ 17.829\ 19.329\ 11.529]\ ml \cdot min^{-1}$ $Q_s = 9.557\ ml \cdot min^{-1}$

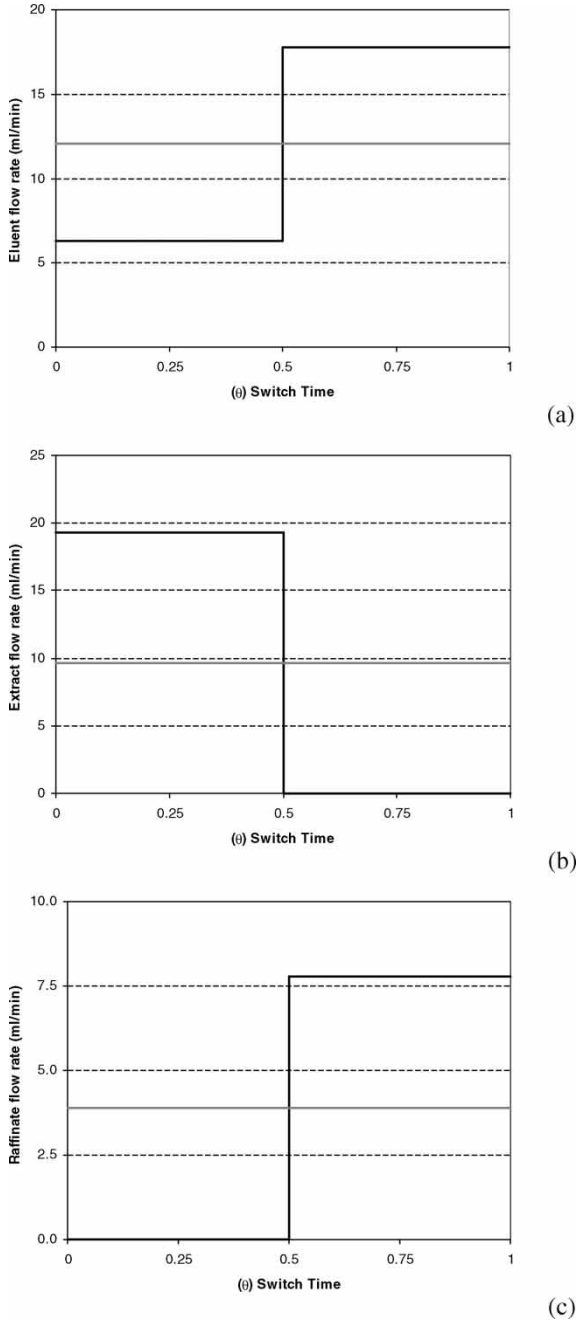

Figure 7. Eluent (a), Extract (b) and Raffinate (c) currents during the pure 50–50% OSS *extract-raffinate* SMB strategy, here operating at 50% of the switch time for each step.

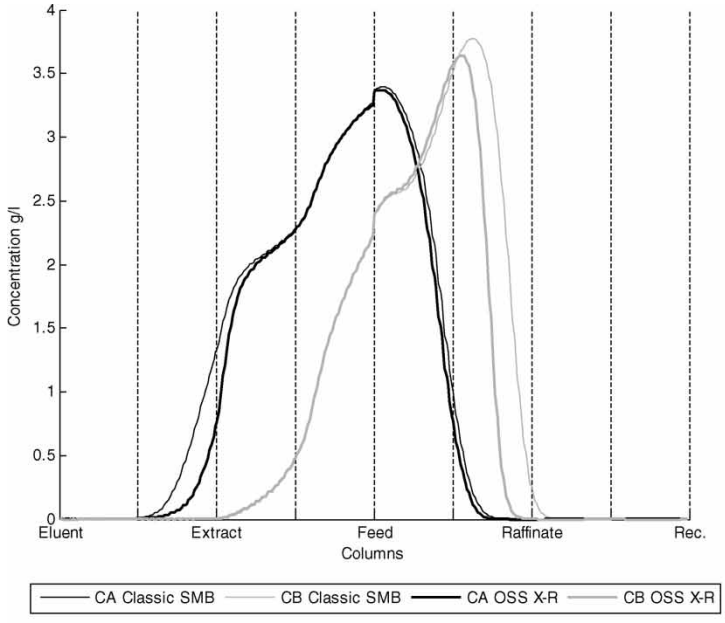

(a)

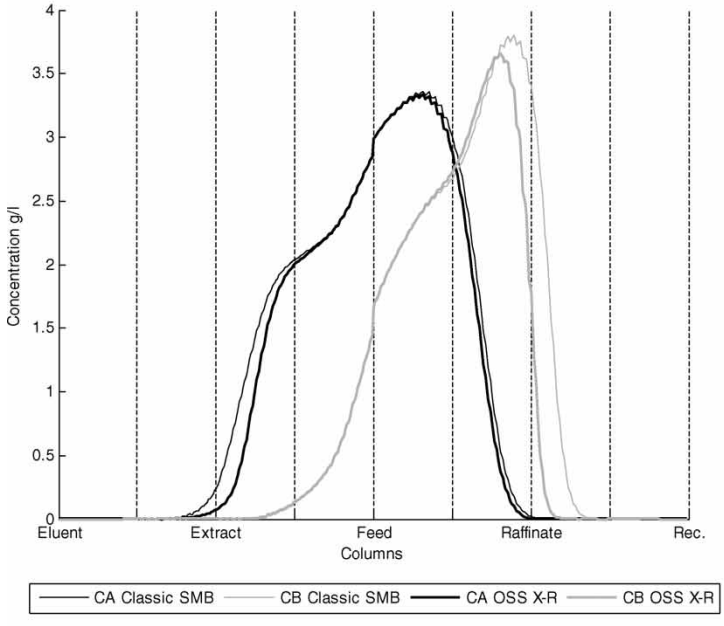

(b)

Figure 8. Concentration profiles for the pure OSS 50–50% extract-raffinate strategy, (a) at $\theta = 0.23$ and (b) at $\theta = 0.73$, at the CSS.

($Q_F = 1.500\ \text{ml} \cdot \text{min}^{-1}$) presented similar purity values in both the extract and the raffinate as the case study here the so-called classic SMB ($P_X = 99.1\%$ of A and $P_R = 98.5\%$ of B). A summary of these operating conditions and model parameters is presented in Tables 1 and 2.

The OSS is limited by the complete closing of the extract and/or raffinate ports. Considering that each step is performed for 50% of the switch time, in the left extreme we have the pure 50-50% OSS-*extract-raffinate* strategy, where in the first step a complete closure of the raffinate port is performed and the same in step 2 for the extract port; in the middle the classic operation and in the right limit the pure 50-50% OSS-*raffinate-extract*, as seen in Fig. 5:

This study particularly analyses the pure strategies mentioned above, and compares it with the classic SMB approach.

OSS Extract-Raffinate Strategy

For the first approach we can consider the simple case pure 50-50% OSS extract-raffinate strategy of a SMB where the A or B front expansion movement in Section 1 or 4 is obtained by closing the raffinate outlet leaving the extract flow-rate higher than the estimated by the classic approach, during the first half of the switch time; and closing the extract outlet while leaving the raffinate flow-rate bigger than estimated by the classic approach during the other half of the switch time, respectively. This is presented in Fig. 6, and the operating values are shown in Table 3, and the flow-rates of the outlet and inlet streams are detailed in Fig. 7.

With the operating parameters above, the stretched profiles are obtained as mentioned before, modelled by the real SMB with LDF approach, as in Fig. 8.

The eluent consumption in the classic approach is $12.038\ \text{ml} \cdot \text{min}^{-1}$, and with the OSS approach also $12.038\ \text{ml} \cdot \text{min}^{-1}$ of eluent not constantly but periodically, during the first step $17.776\ \text{ml} \cdot \text{min}^{-1}$ and the second half time (step 2) $6.300\ \text{ml} \cdot \text{min}^{-1}$. However, when it concerns the purity and the recovery values, it is quite different as can be observed in Table 4:

Table 4. Values for extract and raffinate purity and recovery for the 50-50% OSS *extract-raffinate* technique and the classical SMB separation

	Classic SMB		OSS Technique	
	Extract	Raffinate	Extract	Raffinate
Purity	99.1% of *A*	98.5% of *B*	99.0% of *A*	98.5% of *B*
Recovery	98.5% of *A*	99.1% of *B*	98.5% of *A*	99.0% of *B*

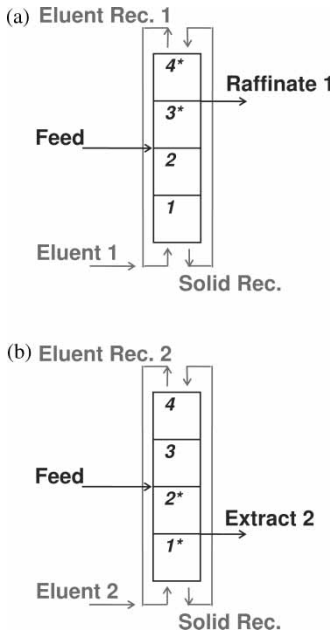

Figure 9. OSS strategy for the test case, (a) the first half of the switch time, (b) the second half of the switch time, equivalent TMB scheme.

OSS Raffinate-Extract Strategy

Now the other possible configuration, working with the same flow-rates and the same step time (50% of the real switch time), where the collection on the extract is during the second stage (step 2) and the collection of the less

Table 5. 50-50% OSS *raffinate-extract* SMB and equivalent TMB section operating conditions

Real SMB 1st half of a θ	Equivalent TMB 1st half of a θ
$\gamma_j^* = [3.798\ 3.798\ 4.034\ 2.809]$ $Q_j^* = [24.200\ 24.200\ 25.700\ 17.900]\ \text{ml} \cdot \text{min}^{-1}$	$\gamma_j = [2.798\ 2.798\ 3.034\ 1.809]$ $Q_j = [17.829\ 17.829\ 19.329\ 11.529]\ \text{ml} \cdot \text{min}^{-1}$ $Q_s = 9.557\ \text{ml} \cdot \text{min}^{-1}$
Real SMB 2nd half of a θ $\gamma_j^* = [6.824\ 3.798\ 4.034\ 4.034]$ $Q_j^* = [43.476\ 24.200\ 25.700\ 25.700]\ \text{ml} \cdot \text{min}^{-1}$	Equivalent TMB 2nd half of a θ $\gamma_j = [5.824\ 2.798\ 3.034\ 3.034]$ $Q_j = [37.105\ 17.829\ 19.329\ 19.329]\ \text{ml} \cdot \text{min}^{-1}$ $Q_s = 9.557\ \text{ml} \cdot \text{min}^{-1}$

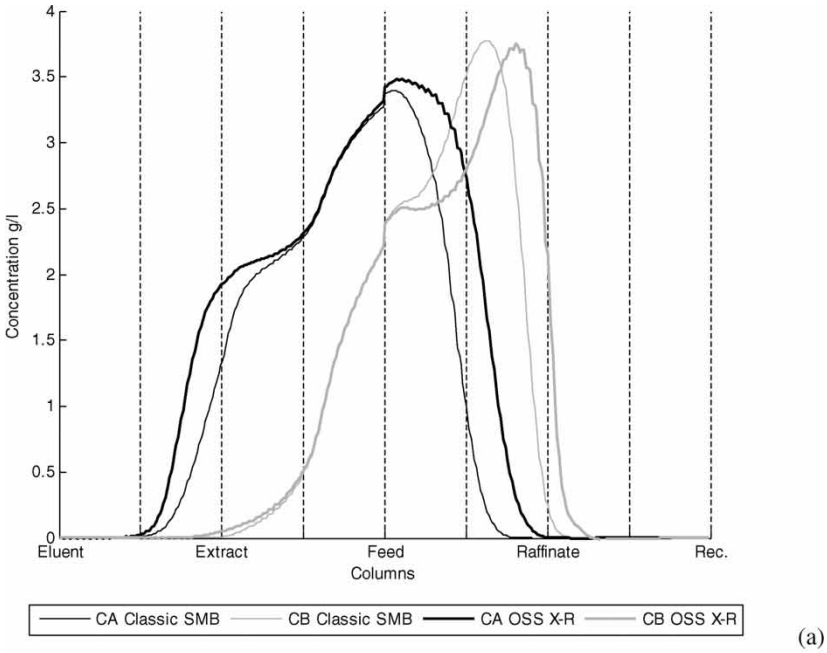

(a)

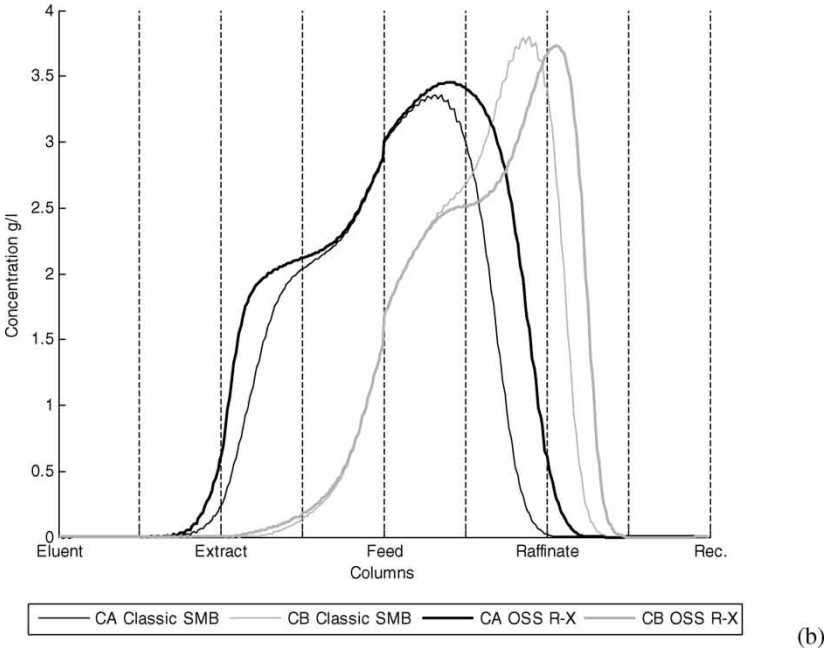

(b)

Figure 10. Concentration profiles for the pure OSS 50-50% raffinate-extract strategy, (a) at $\theta = 0.23$ and (b) at $\theta = 0.73$, at the CSS.

retained product in the raffinate during the first stage (step 1), Fig. 9, and the operating values in Table 5. Simulation results for the concentration profiles at $\theta = 0.23$ and $\theta = 0.73$ at CSS are shown in Fig. 10.

Again the eluent consumption in the classic approach is the same as in the OSS raffinate-extract, not constantly but periodically, during the first step $6.300\ \text{ml} \cdot \text{min}^{-1}$ and the second half time (step 2) $17.776\ \text{ml} \cdot \text{min}^{-1}$. The performance parameters for this strategy are shown in Table 6:

OSS Strategies Evaluation

As can be observed the second strategy presented (pure 50–50% OSS *raffinate-extract*), is quite better than the classic SMB unit as for the other OSS strategy. A good presentation of the technique performance is achieved with the species recovering in outlet streams here exemplified by the concentration history in the extract for both species analyzed, Figure 11:

As noted, the amount of species A is similar in both OSS strategies as in the classical approach; nevertheless, there are important differences in the B species, the contamination front, as can be seen in Fig. 11(b), where the 50–50% OSS *raffinate-extract* technique justifies why the values of the purities in the extract have been improved.

MULTIFEED (MF) OPERATION OF SMBS

Similar to the multiple feed distillation, the use of more than one feed stream in an SMB unit, here called MultiFeed, reveals some interesting results. This type of configuration is presented here as one SMB unit where feed is performed by 2 or more inlet feed streams, between the extract and raffinate outlet collection points, generally part of the single feed current in the equivalent classic SMB, resulting in a sort of a "distributed feed." This assumption leads to the formation of "sub-sections" in the

Table 6. Values for extract and raffinate purity and recovery for the 50–50% OSS *raffinate-extract* technique and the classical SMB separation

	Classic SMB		Nome technique	
	Extract	Raffinate	Extract	Raffinate
Purity	99.1% of *A*	98.5% of *B*	99.7% of *A*	98.6% of *B*
Recovery	98.5% of *A*	99.1% of *B*	98.6% of *A*	99.7% of *B*

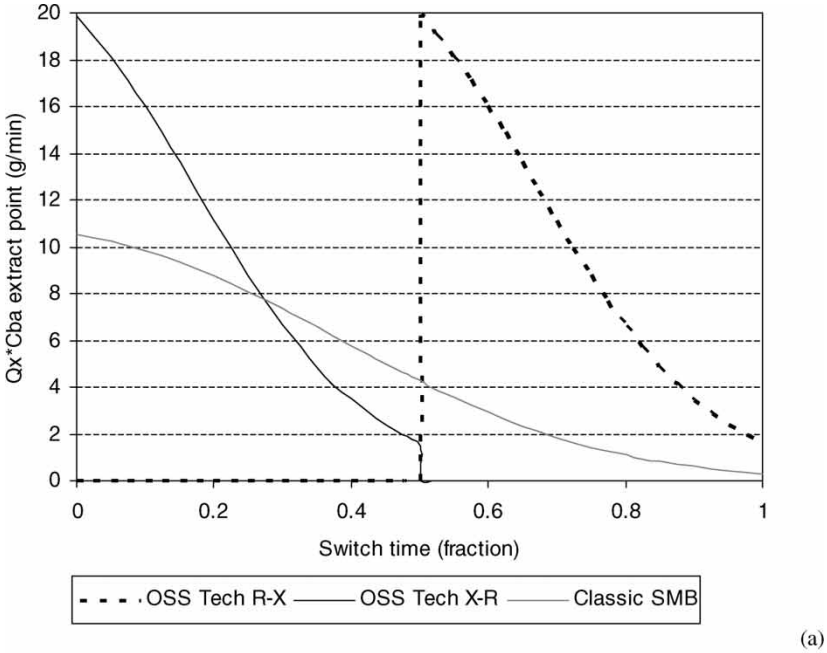

(a)

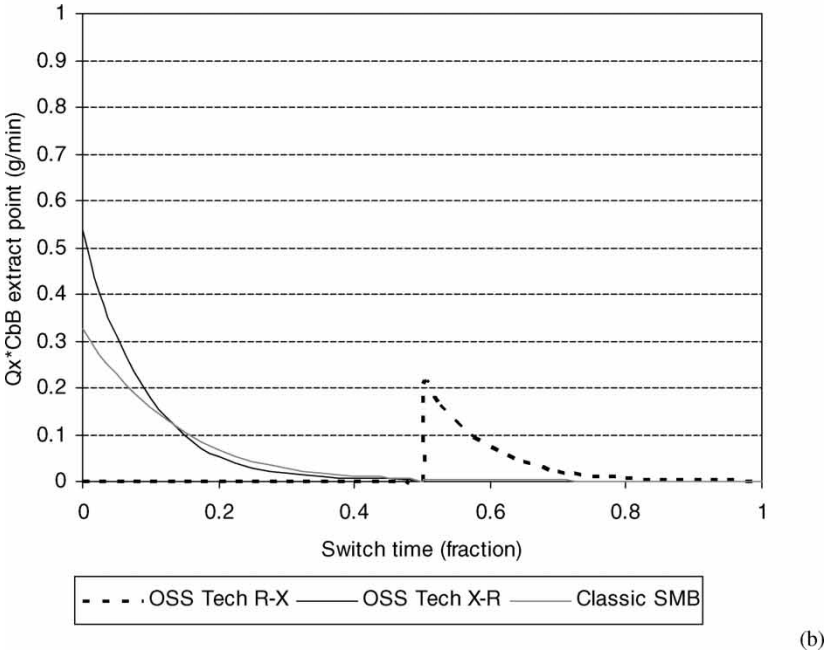

(b)

Figure 11. Concentration history in the extract stream (a) A species and (b) de B species.

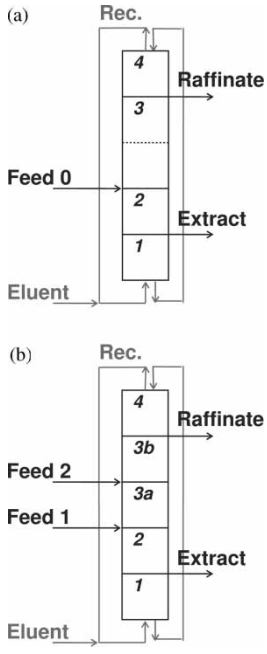

Figure 12. Classic [1-1-2-1] SMB unit scheme (a) and the [1-1-1-1-1] MultiFeed SMB unit scheme (b).

classic zone 3, one for each of the new partial feeds. As example let us consider the classic SMB [1-1-2-1] configuration Fig. 12(a), there is a possibility to split the feed (Feed 0) into two partial feeds (Feed 1 and Feed 2) Fig. 12(b), since zone 3 has 2 columns, that would lead to the new

Table 7. Varicol® unit characteristics and model parameters

Model parameters	SMB columns
$Pe_c = 1600$	N_c=5 $n_j = [1\ 1.5\ 1.5\ 1]$
$\varepsilon_b = 0.4$;	$L_c = 15.84 \times 10^{-2}$ m
$R_p = 2.25 \times 10^{-5}$ m	$d_c = 2.6 \times 10^{-2}$ m
	SMB operating conditions
	$C_A^F = 5\ g \cdot l^{-1}$
$k_{LDF} = 0.4\ s^{-1}$	$C_B^F = 5\ g \cdot l^{-1}$
	$t_c = 316.8$ s
	$Q_E = 25.033\ ml \cdot min^{-1}$
	$Q_X = 17.343\ ml \cdot min^{-1}$
	$Q_F = 0.637\ ml \cdot min^{-1}$
	$Q_R = 8.327\ ml \cdot min^{-1}$
	$Q_4 = 17.794\ ml \cdot min^{-1}$

Table 8. Varicol® real SMB and equivalent TMB section operating conditions

Real SMB	Equivalent TMB
$\gamma_j^* = [6.722\ 4.000\ 4.100\ 2.793]$	$\gamma_j = [5.722\ 3.000\ 3.100\ 1.793]$
$Q_j^* = [42.827\ 25.484\ 26.121\ 17.794]\ \text{ml} \cdot \text{min}^{-1}$	$Q_j = [36.456\ 19.113\ 19.750\ 11.423]\ \text{ml} \cdot \text{min}^{-1}$
	$Q_s = 9.556\ \text{ml} \cdot \text{min}^{-1}$

configuration [1-1-1-1-1], and the formation of two new "sub-sections" in the former zone 3, "sub-section 3a and 3b," each one with one column, becoming something as illustrated in Fig. 12(b).

For the MultiFeed test case the model parameters and operating conditions, were taken from Pais and Rodrigues (6), where the classic interstitial velocity ratios values (γ_j^* or γ_j) for Sections 1 and 4 were kept constant and far from the critical values for the total solid and eluent regeneration in Section 4 and 1 respectively agreeing with the equilibrium theory. For

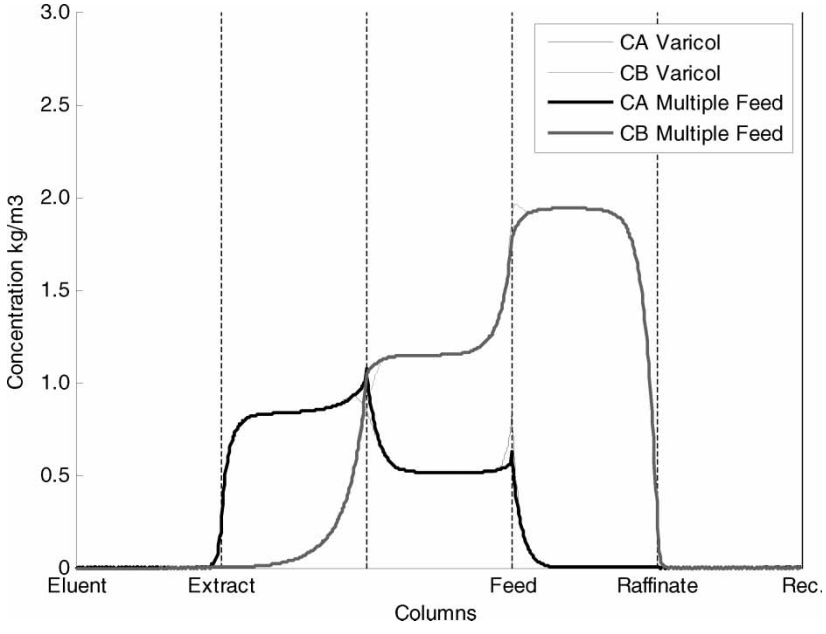

Figure 13. MultiFeed versus Varicol® (second half of the switch time) bulk concentration profiles, for the equivalent TMB with LDF approximation model solutions at cyclic steady-state.

Sections 2 and 3 the interstitial velocity ratios were taken from the analysis presented in (6) based on the ($\gamma_3 \times \gamma_2$) separation region for a 99.0% purity criterion with mass transfer coefficient of $k_{LDF} = 0.4\ s^{-1}$, a summary for these operating conditions and model parameters is presented in Tables 7 and 8.

A particular case appears when the two new feeds have the same value as Feed 0 in the classic SMB, Feed 1 = Feed 2 = Feed 0, but operating in a discontinuous mode by *switching on* one when the other is *switched off* and *vice-versa*. This type of operation will reflect the same *modus operandi* of the equivalent Varicol® scheme, in this case the [1-1.5-1.5-1] configuration. Quite interesting is the fact that when the MultiFeed configuration is set to continuous being Feed 1 = Feed 2 = 1/2(Feed 0) as shown in Fig. 12(b) the TMB solution, compared with the equivalent TMB Varicol® [1-1.5-1.5-1] configuration, with Feed 0 = Feed 1 + Feed 2, reproduces the same results in terms of bulk concentration in the regions around the extract and raffinate collection points as presented in Fig. 13. The same conclusion was observed by Kim et al. (14), and in fact Varicol®, with only inner variable number of columns (in Sections 2 and 3), can be considered as a particular case of the multiple feed SMB operation strategy. Therefore, one can expect that the "triangle" separation region could be the same for Varicol® and MF in the same conditions.

Reminding all the optimum feeds location in the multiple feed distillation field as in McCabe and Thiele (42), and establishing a simple equivalence between multiple feed SMB chromatographic processes, allows us to have a powerful methodology for the optimization/development of new SMB processes, in particular the Varicol® technique.

CONCLUSIONS

A new non-conventional SMB technique was introduced, modelled, and simulated the outlet streams swing (OSS). The new technique, was compared with the classical SMB optimized approach in the same Chiral separation system leading to outlet streams purities improvements, when modelled by the real SMB method considering the linear driving force approximation to the particle mass transfer, solved by the commercial package gPROMS. Further work shall be presented mainly regarding the study of OSS operating parameters, as the step distribution time, the utilization of extract and raffinate partial flow-rates, and consequent optimization.

Also the simulation of the MultiFeed technique proved to be a solo valuable new technique in the SMB process as a powerful design/optimization procedure for some particular cases of the already well known non-conventional technique, the Varicol®, namely the only inner zones variable number of columns.

NOTATION

C_b	bulk fluid phase concentration ($mol \cdot m^{-3}$)
C^F	feed concentration ($mol \cdot m^{-3}$)
$\langle q \rangle$	average pores particle adsorbent fluid phase concentration ($mol \cdot m_{solid}^{-3}$)
D_b	axial dispersion coefficient ($m^2 \cdot s^{-1}$)
D_{pe}	effective pore diffusion coefficient ($m^2 \cdot s^{-1}$)
d_c	column diameter (m)
L_c	column axial length (m)
L_j	section axial length (m)
NC	total number of columns)
n_j	number of columns per section
P	purity (%)
Pe	Peclet number
Pro	unit productivity ($g \cdot (s \cdot m_{solid}^3)^{-1}$)
Q	fluid/solid flowrate ($m^3 \cdot s^{-1}$)
q^*	solid retained concentration ($mol \cdot m_{solid}^{-3}$)
Rec	recovery (%)
R_p	particle radius (m)
k_p	dimensionless mass transfer coefficient
k_{LDF}	particle LDF approach mass transfer coefficient (s^{-1})
V_c	column volume (m^3)
t	time variable (s)
t_j	bulk fluid space time (s)
t_c	solid space time (switch time) (s)
u_j	interstitial fluid velocity in section j ($m \cdot s^{-1}$)
u_s	solid interstitial counter-current velocity ($m \cdot s^{-1}$)
x	dimensionless axial column coordinate)
z	axial column coordinate (m)

Greek Letters

γ	ratio between fluid and solid interstitial velocities
ε_b	bed porosity
θ	dimensionless time coordinate

Indexes

*	in the real SMB model
A	more retained species
B	less retained species
b	bulk
p	particle
s	solid

c	column
i	chemical species
j	SMB section
E	eluent stream
F	feed stream
R	raffinate stream
X	extract stream

Abbreviations

AE	Algebraic equations
CSS	Cyclic steady state
DAE	Differential-algebraic equations
LDF	Linear driving force
MF	MultiFeed SMB
OCFEM	Orthogonal collocation in finite elements method
ODE	Ordinary differential equations
OSS	Outlet streams swing SMB
PDAE	Partial differential algebraic equations
PDE	Partial eifferential equations
SMB	Simulated moving bed
TMB	True moving bed

ACKNOWLEDGEMENTS

Pedro Sá Gomes acknowledges the financial support from FCT "Fundação para a Ciência e a Tecnologia" (Ph-D grant SFRH/BD/22103/2005), Ministry of Science and Technology of Portugal. Financial support through the project POCI/EQU/59296/2004 is gratefully acknowledged.

REFERENCES

1. Broughton, D.B. and Gerhold, C.G. (1961) Continuous Sorption Process Employing Fixed Bed of Sorbent and Moving Inlets outlets. U.S. Patent No. 2,985,589.
2. Pavone, D. and Hotier, G. (2000) System approach modelling applied to the eluxyl process. *Revue IFP*, 55: 437.
3. Minceva, M. and Rodrigues, A.E. (2002) Modelling and simulation of a simulated moving bed for the separation of p-xylene. *Ind. Eng. Chem. Research*, 41: 3454–3461.
4. Nicoud, R.M. (1999) The separation of optical isomers by simulated moving bed chromatography. *Pharm. Tech. Europe*, 11 (3): 36.
5. Nicoud, R.M. (1999) The separation of optical isomers by simulated moving bed chromatography. *Pharm. Tech. Europe*, 11 (4): 28.

6. Pais, L.S. and Rodrigues, A.E. (2003) Design of simulated moving bed and varicol processes for preparative separations with a low number of columns. *J. Chromatogr. A*, 1006: 33–44.
7. Rodrigues, A.E. and Pais, L.S. (2004) Design of SMB chiral separations units using concept of separation volume. *Sep. Sci. Tech.*, 39: 245–270.
8. Adam, P.R., Nicoud, M., Bailly, M., and Ludemann-Hombourger, O. (2000) U.S. Patent No 6,136,198.
9. Ludemman-Hombouger, O., Nicoud, R., and Bailly, M. (2000) The "Varicol" process: a new multicolumn continuous chromatographic process. *Sep. Sci. Tech.*, 35 (12): 1829–1862.
10. Morbidelli, M. and Mazzotti, M. (2002) Advances in simulated moving bed chromatography. In *PREP, 15th International Symposium, Exhibit Workshops on Preparative/Process Chromatography Ion Exchange, Adsorption/Desorption Processes & Related Separation Techniques*. Lecture 201. Washington DC, USA, 53–54.
11. Zhang, Z., Mazzotti, M., and Morbidelli, M. (2003) PowerFeed operation of simulated moving bed units: changing the flow-rates during the switching interval. *J. Chromatogr. A*, 1006 (1&2): 87–99.
12. Schramm, H., Kaspereit, M., Kienle, A., and Seidel-Morgenstern, A. (2002) Improving simulated moving bed processes by cyclic modulation of the feed concentration. *Chem. Eng. Tech.*, 25 (12): 1151–1155.
13. Schramm, H., Kaspereit, M., Kienle, A., and Seidel-Morgenstern, A. (2003) Simulated moving bed process with a cyclic modulation of the feed concentration. *J. Chromatogr. A*, 1006: 77–86.
14. Kim, J.K., Abunasser, N., and Wankat, P.C. (2005) Use of two feeds in simulated moving beds for binary separation. *Korean J. Chem. Eng.*, 22 (4): 619–627.
15. Hashimoto, K., Adachi, S., Shirai, Y., and Morishita, M. (1993)) Operation and design of simulated moving bed adsorbers. In *Preparative and Production Scale Chromatogr*; Ganetsos, G. and Barker, P.E. (eds.); Marcel Dekker: New York, 273–300.
16. Balannec, B. and Hotier, G. (1993)) From batch elution to simulated countercurrent chromatography. In *Preparative and Production Scale Chromatography*; Ganetsos, G. and Barker, P.E. (eds.); Marcel Dekker: New York, 301–357.
17. Kearney, M. and Hieb, K.L.U.S. Patent No. 5,102,553.
18. Beste, Y.A. and Arlt, W. (2001) Simulated countercurrent chromatography with sidestream discharge. *Chemie-Ingenieur Technik*, 73: 1567–1572.
19. Kim, J.K., Zang, Y.F., and Wankat, P.C. (2003) Single-cascade simulated moving bed systems for the separation of ternary mixtures. *Ind. Eng. Chem. Research*, 42: 4849–4860.
20. Kishihara, S., Fujii, S., Tamaki, H., Kim, K.B., Wakiuchi, N., and Yamamoto, T. (1992) Continuous chromatographic-separation of sucrose, glucose, and fructose using a simulated moving bed adsorber. *Int. Sugar J.*, 94: 305–308.
21. Wooley, R., Ma, Z., and Wang, N.-H.L. (1998) A nine-zone simulating moving bed for the recovery of glucose and xylose from biomass hydrolyzate. *Ind. Eng. Chem. Research*, 37: 3699–3709.
22. Masuda, T., Sonobe, T., Matsuda, F., Horie, M. (1993) Process for fractional separation of multi-component fluid mixtures. U.S. Patent No. 5,198,120.
23. Mata, V.G. and Rodrigues, A.E. (2001) Separation of ternary mixtures by pseudo-simulated moving bed chromatography. *J. Chromatogr. A*, 23: 939.

24. Borges da Silva, E.A. and Rodrigues, A.E. (2006) Methodology for the design of chromatographic multicomponent separation by a pseudo-simulated moving bed. *AIChE J.*, 52 (11): 3794–3812.
25. Sá Gomes, P., Leão, C.P., and Rodrigues, A.E. (2006) Simulation of true moving bed adsorptive reactor: detailed particle model and linear driving force approximations. Submitted to *Chem. Eng. Sci.* in press.
26. Glueckauf, E. (1955) Theory of chromatography Part 10: formula for diffusion into spheres and their application to chromatography. *Trans. Faraday Soc.*, 51: 1540–1551.
27. Danckwerts, P.V. (1953) Continuous flow systems; distribution of residence times. *Chem. Eng. Sci.*, 2: 2.
28. Langmuir, I. (1908) The velocity of reactions in gases moving through heated vessels and the effect of convection and diffusion. *J. Am. Chem. Soc.*, 30: 1742–1754.
29. DeVault, D. (1943) The theory of chromatography. *J. Am. Chem. Soc.*, 65: 532.
30. Helfferich, F. and Klein, G. (1970)) *Multicomponent Chromatography*; Marcel Dekker: New York.
31. Helfferich, F.G. (1967) Multicomponent ion exchange in fixed beds: generalized equilibrium theory for systems with constant separation factors. *Ind. Eng. Chem. Fundamentals*, 6 (3): 362–364.
32. Klein, G., Tondeur, D., and Vermeulen, T. (1967) Multicomponent ion exchange in fixed beds: general proprieties of equilibrium systems. *Ind. Eng. Chem. Fundamentals*, 6 (3): 339–351.
33. Rhee, H.-K., Aris, R., and Amundson, N.R. (1970) On the theory of multicomponent chromatography. *Phil. Trans. Roy. Soc. London A*, 296: 419.
34. Tondeur, T. and Klein, G. (1967) Constant-separation-factor equilibrium. *Ind. Eng. Chem. Fundamentals*, 6 (3): 351–361.
35. Storti, G., Masi, M., Carrá, S., and Morbidelli, M. (1989) Optimal design of multicomponent counter-current adsorption separation processes involving nonlinear equilibria. *Chem. Eng. Sci.*, 44: 1329–1345.
36. Storti, G., Mazzotti, M., Morbidelli, M., and Carrá, S. (1993) Robust design of binary counter-current adsorption separation processes. *AIChE J.*, 39: 471–492.
37. Mazzotti, M., Storti, G., and Morbidelli, M. (1997) Optimal operation of simulated moving bed units for nonlinear chromatographic separations. *J. Chromatogr. A*, 769: 3–24.
38. Chiang, A.S.T. (1998) Equilibrium theory for simulated moving bed adsorption processes. *AIChE J.*, 44 (11): 2431–2441.
39. Migliorini, C., Mazzotti, M., and Morbidelli, M. (2000) Design of simulated moving bed multicomponent separations: langmuir systems. *Separation and Purification Technology.*, 20: 79–96.
40. Azevedo, D.C. and Rodrigues, A.E. (1999) Design of a simulated moving bed in the presence of mass-transfer resistances. *AIChE J.*, 45: 959.
41. Minceva, M. and Rodrigues, A.E. (2005) Two-level optimization of an existing SMB for p-xylene. *Separation Comp. Chem. Eng.*, 29: 2215–2228.
42. McCabe, W.L. and Thiele, E.W. (1925) Graphical design of fractionating columns. *Ind. Eng. Chem.*, 17: 605.